C. R. Mecanique 338 (2010) 121–126

Contents lists available at ScienceDirect

Comptes Rendus Mecanique

www.sciencedirect.com

Mixed-mode crack propagation using a Hybrid Analytical and eXtended Finite Element Method

Propagation de fissure en mode mixte par une méthode d'éléments finis hydride

Julien Réthoré [a,*], Stéphane Roux [b], François Hild [b]

[a] *LaMCoS, Université de Lyon/INSA Lyon/CNRS, 20, avenue des sciences, 69621 Villeurbanne cedex, France*
[b] *LMT-Cachan, ENS de Cachan/CNRS/UPMC/PRES UniverSud Paris, 61 avenue du Président Wilson, 94235 Cachan cedex, France*

ARTICLE INFO

Article history:
Received 4 September 2009
Accepted 4 March 2010
Available online 27 March 2010

Keywords:
Rupture
Crack propagation
Extended Finite Element Method
Analytical model

Mots-clés :
Rupture
Propagation de fissure
Méthode des éléments finis étendus
Méthode analytique

ABSTRACT

A Hybrid Analytical and eXtended Finite Element Method (HAX-FEM) is proposed to study the propagation of curved mixed-mode cracks. A Double Edge Notched test on a concrete sample is simulated. A specific treatment is proposed to account for crack initiation from a finite width notch. The crack morphology is in good agreement with previously published experimental results.

RÉSUMÉ

Une méthode hybride analytique et éléments finis étendus est utilisée pour étudier la propagation de fissures courbes en mode mixte. Un essai sur un spécimen doublement entaillé est simulé. Un traitement spécifique de l'amorçage de la fissure à partir d'une entaille large est proposé dans le cadre de cette méthode. La trajectoire de la fissure est en bon accord avec des résultats expérimentaux de la littérature.

1. Introduction

Many strategies are available for the numerical simulation of crack propagation for complex loadings and geometries. The challenge is thus no longer on the feasibility of such computations, but rather on the simplicity of the methodology, its flexibility and performance. In this spirit, the eXtended Finite Element Method (X-FEM) [1] has shown definite advantages over other techniques such as adaptive remeshing since only the vicinity of the crack path supports specific enrichments.

Recently, another method has been proposed by the authors that partly relies on X-FEM away from the crack tip. Only the treatment of the near-tip region differs. The latter is described by analytical fields derived from linear elastic fracture mechanics (LEFM), which directly provide a precise evaluation of Stress Intensity Factors (SIFs). These two descriptions are coupled over an overlapping region to ensure a full consistency through Lagrange multipliers. This method was referred to as "Hybrid Analytical/eXtended Finite Element Method" or HAX-FEM. A detailed study of the performance of this method in terms of SIF evaluation as a function of the size of the enriched crack tip region, overlapping zone, and degree of enrichment was published recently [2].

* Corresponding author.
E-mail addresses: julien.rethore@insa-lyon.fr (J. Réthoré), stephane.roux@lmt.ens-cachan.fr (S. Roux), francois.hild@lmt.ens-cachan.fr (F. Hild).

1631-0721/$ – see front matter
doi:10.1016/j.crme.2010.03.001

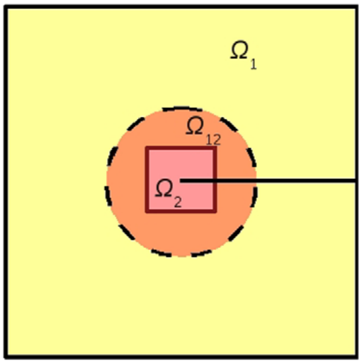

Fig. 1. Schematic description of the domains considered in HAX-FEM: Ω_1 is described using X-FEM, Ω_2 using Williams' series and Ω_{12} is the coupling zone.

The purpose of the present contribution is to apply this strategy to a documented experimental case, a Double Edge Notched (DEN) concrete specimen subjected to a multi-axial loading. Two symmetric (up to experimental uncertainties) curved cracks develop because of mixed-mode loading. It is therefore a good candidate to validate the reliability of the method for handling propagation in a complex test. Incidently, this test has been frequently used as a benchmark for different approaches, not only for the numerical simulation methodology, but also for the relevant mechanical description. In particular, damage mechanics is severely challenged since the failure mode is essentially a *damage localization*, which is well known for numerical stability and objectivity issues [3]. A fracture mechanics description is free from these difficulties, and as such, may be considered as a simple alternative to more sophisticated non-linear constitutive laws to model such tests.

Section 2 briefly presents the HAX-FEM methodology. The case study (DEN test) is introduced in Section 3. A specific treatment of crack initiation is proposed in Section 3.2 to account for the finite width notch of the experiment. Last, the results are compared to experimental observations in Section 4.

2. Problem formulation

Let us consider a homogeneous body with an isotropic and elastic behavior, and a 2D setting. The displacement field $\boldsymbol{u}$ is conventionally represented by its complex writing, $\boldsymbol{u} = u_x + iu_y$. It was expanded by Williams [4] for a straight crack as a double series of $\boldsymbol{\phi}_i^n$ linear elastic fields satisfying a zero traction condition along the crack path

$$\boldsymbol{\phi}_I^n(r,\theta) = r^{n/2}\left[\kappa e^{in\theta/2} - \frac{n}{2}e^{i(4-n)\theta/2} + \left(\frac{n}{2} + (-1)^n\right)e^{-in\theta/2}\right] \tag{1}$$

and

$$\boldsymbol{\phi}_{II}^n(r,\theta) = ir^{n/2}\left[\kappa e^{in\theta/2} + \frac{n}{2}e^{i(4-n)\theta/2} - \left(\frac{n}{2} - (-1)^n\right)e^{-in\theta/2}\right] \tag{2}$$

where κ is Kolossov's constant, namely, $\kappa = (3-\nu)/(1+\nu)$ for plane stress or $\kappa = (3-4\nu)$ for plane strain conditions, ν being Poisson's ratio. This family of fields is the appropriate basis to describe the displacement field for a traction free crack in an elastic body.

In Ref. [2], a two-description strategy is proposed for the displacement field. In the vicinity of the crack tip (Ω_2 in Fig. 1), the displacement field $\boldsymbol{u}_2(\boldsymbol{x})$ reads

$$\boldsymbol{u}_2(\boldsymbol{x}) = \frac{1}{2\mu\sqrt{2\pi}} \sum_{n\in[0;\, n_{\max}]} \boldsymbol{\phi}_I^n(\boldsymbol{x})\, p_n + \boldsymbol{\phi}_{II}^n(\boldsymbol{x}) q_n = \boldsymbol{\Phi}^T \boldsymbol{U}_2 \tag{3}$$

where μ is Lamé's coefficient, p_n and q_n the degrees of freedom associated with mode I and II functions, and $n_{\max}$ an integer that defines the maximum order considered in the interpolation. Note that for $n=1$, p_1 and q_1 provide a direct evaluation of K_I and K_{II} without any further post-processing as usually required by FEM or X-FEM simulations (*e.g.* [5]).

Away from the crack tip (Ω_1 in Fig. 1), the displacement field $\boldsymbol{u}_1(\boldsymbol{x})$ is discretized using an X-FEM kinematics [1]

$$\boldsymbol{u}_1(\boldsymbol{x}) = \sum_{i\in\mathcal{N}_1} \boldsymbol{N}_i(\boldsymbol{x}) d_i + \sum_{i\in\mathcal{N}_{cut}} \boldsymbol{N}_i(\boldsymbol{x})\mathcal{H}(\boldsymbol{x}) b_i = \boldsymbol{D}^T \boldsymbol{U}_1 \tag{4}$$

where $\boldsymbol{N}_i$ are standard finite element shape functions supported by the set of nodes $\mathcal{N}_1$ included in Ω_1^h, d_i the corresponding degrees of freedom. In this equation, $\mathcal{H}(\boldsymbol{x})$ is the discontinuous symmetrized Heaviside step function (with its associated degrees of freedom b_i) that enables for the description of displacement discontinuities for the nodes in the subset $\mathcal{N}_{cut}$ of $\mathcal{N}_1$ whose support is cut by the crack.

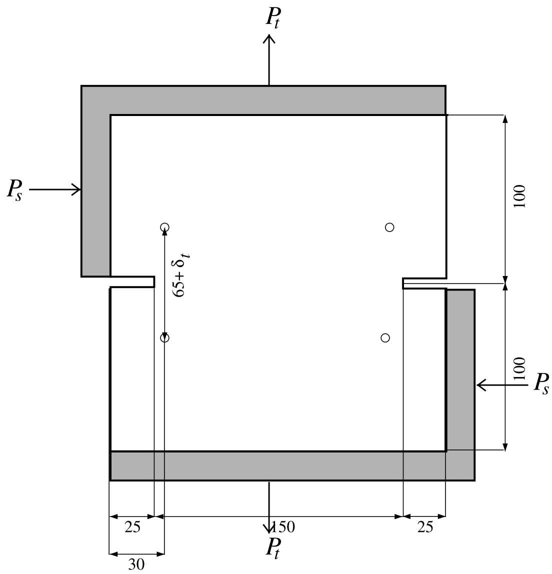

Fig. 2. Setup of Nooru-Mohamed's experiment [7].

These two descriptions are coupled using the Arlequin method [6] over Ω_{12}. The principle is that the two models share the strain energy density over the overlapping zone and the displacements are coupled in a weak sense using Lagrange multipliers. This hybrid analytical and extended finite element technique was shown to have high order convergence rate in terms of stress intensity factors that are obtained *without resorting to any post-processing step* [2].

3. Simulation of Nooru-Mohamed's experiment

In the following, it is proposed to use HAX-FEM to simulate crack initiation and propagation in a brittle material.

3.1. Setup

The experiments considered herein are based on a Double Edge Notched (DEN) geometry [7]. The latter is square shaped, the width is 200 mm, and the thickness 50 mm. The pre-notches are 25-mm long, and 5-mm thick. The samples are made of unreinforced concrete whose elastic properties are its Young's modulus $E = 30$ GPa, and its Poisson's ratio $\nu = 0.2$. A mixed-mode loading is applied to the specimen as described by Fig. 2. The shear load is maintained to a constant value P_s, while the tensile load P_t is progressively increased. The mixed mode can be varied by increasing P_s. In this paper, we will focus on a shear load of 10 kN that corresponds to the experiment labeled 4b in Ref. [7].

For the numerical model a regular mesh made of 49×49 quadrangular elements is used. The typical element size h is thus about 4.1 mm. The half width of the analytical model Ω_2 is $5h$ (or 20.5 mm) including a $2h$ thick coupling zone. The boundary conditions are of Dirichlet type, namely, the rotation of the clamps is fixed, the shear displacement is adjusted so that P_s matches the desired value of 10 kN, and the tensile displacement so that the fracture criterion is reached.

3.2. Initiation

In the experiment, the cracks initiate from squared notches. An LEFM approach may thus not be valid at initiation. However, the hoop stress distribution close to a squared pre-notch is compared to the vicinity of a crack tip for the combined tension/shear loading (the shear preload is 10 kN, and the fracture toughness and the equivalent stress intensity factor are given in the next subsection). For the squared notch, the results are obtained using a very fine mesh (4 times finer than the initial one) over a square shaped region around the pre-crack. The width of this square equals the size of the analytical model. Except on the notch faces that are stress free, Dirichlet boundary conditions coming from the large scale computation are applied on the entire boundary of the fine model. Fig. 3 compares the two hoop stress fields. A good agreement is observed, which is confirmed in Fig. 4. The latter shows the variation of the hoop stress along a circle centered at the notch root, and whose radius is the notch width. Maxima of similar magnitude are obtained for the two models at an angle of 50°. Note that the maximum hoop stress agrees well with the material strength $\sigma_c = 3$ MPa [7].

Further, Fig. 5 shows the normalized amplitudes of the fine FE displacement when projected in a least-squares sense onto the basis functions that are used in the analytical domain for the large scale simulation. The change of the amplitudes for different orders is plotted as a function of the size of the domain that is used for the projection. It is shown that significant differences are obtained for the high order terms 4 and 5 only. These terms having only a large distance influence (they

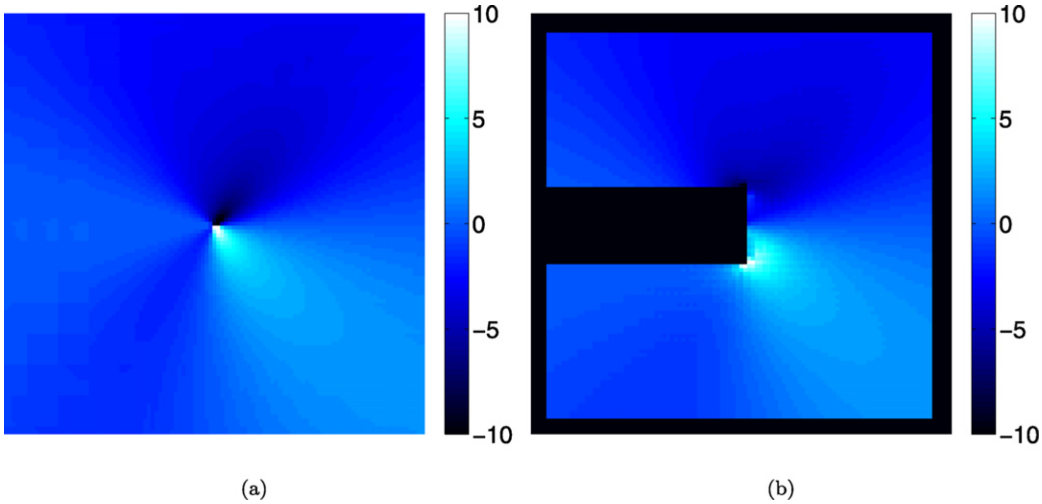

Fig. 3. Hoop stress distribution in MPa around a crack tip using HAX-FEM (a) and around a notch tip using a fine FE model (b) for a combined tension/shear (10 kN) load at initiation.

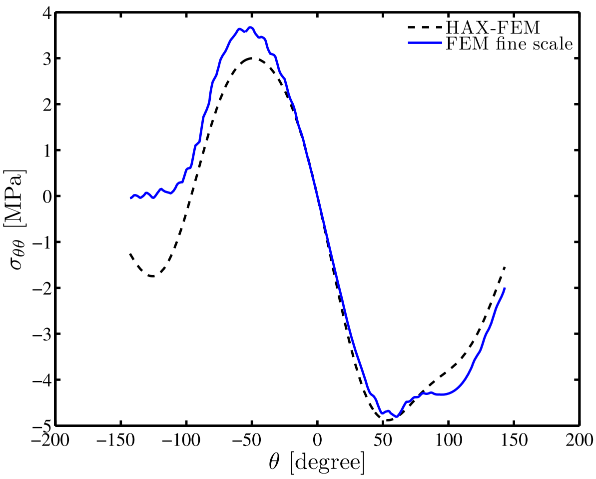

Fig. 4. Comparison of hoop stress distribution along a circle of radius d (the width of the notch) obtained with HAX-FEM and a fine FE model for a combined tension/shear (10 kN) load at initiation.

scale as r^2 and $r^{5/2}$ respectively), one may conclude that the small distance field due to square notch is well approximated using a crack displacement field. A stress criterion applied to the crack tip field of the large scale simulation at a distance d (equal to the notch width) to the crack tip will thus be applied at initiation.

3.3. Crack propagation

During crack propagation, a brittle fracture criterion is used. The fracture toughness of the material is set to 1 MPa$\sqrt{\text{m}}$. The crack propagation angle θ_c and the equivalent stress intensity factor K_I^{eq} are given by the maximum hoop stress criterion

$$\theta_c = 2\tan^{-1}\left(\frac{1}{4}\left[\frac{K_I}{K_{II}} + \operatorname{sign}(K_{II})\sqrt{8 + \left(\frac{K_I}{K_{II}}\right)^2}\right]\right) \tag{5}$$

and

$$K_I^{eq} = K_I \cos^3\left(\frac{\theta_c}{2}\right) - \frac{3}{2} K_{II} \cos\left(\frac{\theta_c}{2}\right) \sin\theta_c \tag{6}$$

At each time step, the crack propagates by an increment of $5h$, *i.e.* the half-width of the inner domain (Ω_2). The crack being described using two level sets, its geometry is updated using a Fast Marching Method [8]. Once the level sets are

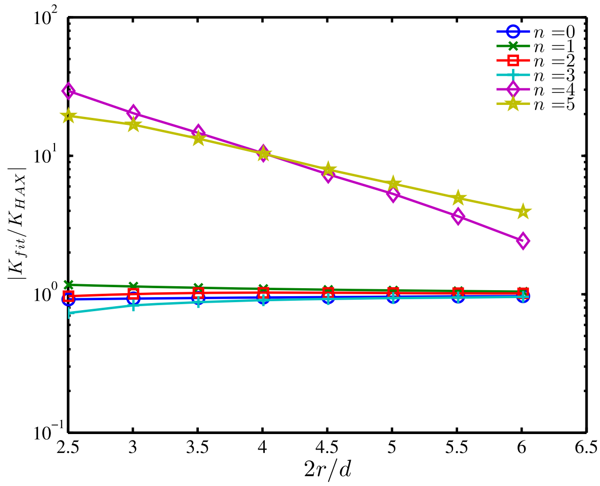

Fig. 5. Ratio between Williams' coefficients obtained by least-squares fit of the fine FE results and those obtained with HAX-FEM for a combined tension/shear loading at initiation. Only mode *I* coefficients are plotted as functions of normalized size of the domain used for the least-squares fit.

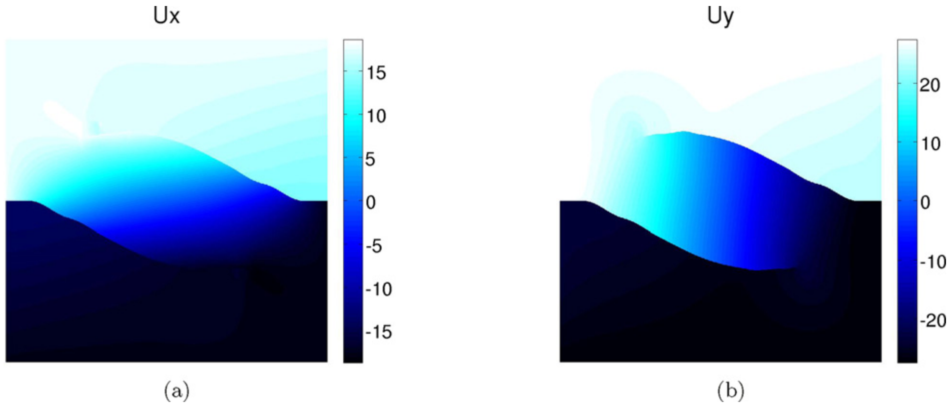

Fig. 6. Horizontal (a) and vertical (b) displacement (in µm) during crack propagation for a shear preload of 10 kN.

updated, the position and orientation of the analytical domain Ω_2 is redefined according to the new position of the crack tip.

One difficulty of the present experiment is that the crack follows a curved trajectory. In the X-FEM region, an arbitrary geometry of the crack path is easily handled by the level sets. However, the fields used in the "analytical" region are those of a straight crack. Thus, in practice the crack path in this region is the secant line joining the crack tip to the intersection of the crack path with the boundary of domain Ω_2. In the present case, the radius of this region is $5h \approx 20.5$ mm, whereas the radius of curvature of the crack trajectory is of the order of 200 mm, and thus the error induced by this simplified geometry is negligible in front of experimental uncertainties. Not only is the geometrical error small, but the fact that the stress vector vanishes on the crack surface further limits the effects of this approximation. To reduce further this effect, it suffices to reduce the extension of the analytic domain Ω_2. A more refined treatment is however possible by computing the analytical fields for slightly curved cracks, as a perturbation expansion. The correction field to Φ^n to first order in the curvature takes a similar form than the higher order fields, with an r-scaling equal to that of Φ^{n+2}. Hence, the very same formalism can easily be extended to significantly curved cracks.

4. Results

Fig. 6 shows the horizontal and vertical displacement fields during crack propagation. One observes the displacement discontinuity along the crack path that is compared to the experimental one in Fig. 7. A good agreement is obtained.

A similar agreement was obtained for other shear preloads, which affect significantly the crack trajectory (orientation and curvature).

It is noteworthy that other modelings of this same experiment based on a damage law are also successful at reproducing the crack pattern and load–displacement curve (see [9–12] among others). Hence we do not pretend that a purely brittle description is more appropriate than a damage law in general for concrete. However for such a test, where damage tends

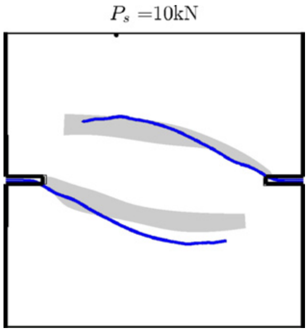

Fig. 7. Comparison of experimental (gray zone) and simulated (thick line) crack paths for $K_{Ic} = 1$ MPa m$^{1/2}$ and a 10-kN shear preload.

to localize onto cracks, an elastic–brittle model is an excellent approximation, and is computationally much easier and less demanding. It is therefore a favorable alternative.

Although the proposed HAX-FEM scheme has the potential of being a very efficient scheme in terms of computation cost, the present implementation of the method has not yet been optimized so that a direct comparison would be unfair. However, the simplicity of the implementation is to be emphasized.

5. Conclusion

The present study has shown the ability of HAX-FEM to deal with mixed-mode crack propagation under multi-axial loading. A good agreement was obtained between the simulation results and the experimental observations. Moreover the crack initiation from a finite width notch is handled within the same framework successfully.

Further extensions of HAX-FEM to account for a cohesive fracture process zone is currently under development and may reveal more relevant for quasi-brittle materials such as concrete or composite materials. However, for the present DEN test, this refinement would essentially affect the initiation step or the very final stage where crack tips interact with the other crack path.

Finally, an optimized implementation is required to reveal quantitatively the numerical efficiency of the HAX-FEM scheme. The simplicity of the implementation is underlined.

Acknowledgements

This work was funded by Agence nationale de la recherche under the grant ANR-09-BLAN-0009-01 (RUPXCUBE Project).

References

[1] N. Moës, J. Dolbow, T. Belytschko, A finite element method for crack growth without remeshing, International Journal for Numerical Methods in Engineering 46 (1) (1999) 133–150.
[2] J. Réthoré, S. Roux, F. Hild, Hybrid analytical and extended finite element method (HAX-FEM): A new enrichment procedure for cracked solids, International Journal for Numerical Methods in Engineering 81 (3) (2010) 269–285.
[3] Z. Bazant, G. Pijaudier-Cabot, Nonlocal continuum damage, localization instability and convergence, Journal of Applied Mechanics 55 (2) (1988) 287–293.
[4] M. Williams, On the stress distribution at the base of a stationary crack, ASME Journal Applied Mechanics 24 (1957) 109–114.
[5] X. Suo, A. Combescure, On the application of the $\mathcal{G}\theta$ method and its comparison with de Lorenzi's approach, Nuclear Engineering and Design 135 (1992) 207–224.
[6] H.B. Dhia, G. Rateau, The Arlequin method as a flexible engineering design tool, International Journal for Numerical Methods in Engineering 62 (2005) 1442–1462.
[7] M. Nooru-Mohamed, Mixed-mode fracture of concrete: An experimental approach, Ph.D. thesis, Delft University of Technology, 1992.
[8] J. Sethian, Level Set Methods and Fast Marching Methods: Evolving Interfaces in Computational Geometry, Fluid Mechanics, Computer Vision, and Material Science, Cambridge University Press, Cambridge, 1996.
[9] R. De Borst, Some recent developments in computational modelling of concrete fracture, International Journal of Fracture 86 (1) (1997) 5–36.
[10] T. Gasser, G. Holzapfel, 3D crack propagation in unreinforced concrete. A two-step algorithm for tracking 3D crack paths, Computer Methods in Applied Mechanics and Engineering 195 (37–40) (2006) 5198–5219.
[11] P. Pivonka, J. Ozbolt, R. Lackner, H. Mang, Comparative studies of 3D-constitutive models for concrete: Application to mixed-mode fracture, International Journal for Numerical Methods in Engineering 60 (2004) 549–570.
[12] B. Patzák, M. Jirásek, Adaptive resolution of localized damage in quasi-brittle materials, Journal of Engineering Mechanics 130 (2004) 720–732.